

## Behavior of a Reverse Lamellar Phase in the Presence of Low Molecular Weight Triblock Molecules

N. Taulier,<sup>\*,†</sup> R. Ober,<sup>‡</sup> M.-F. Gouzy,<sup>§</sup> B. Guidetti,<sup>§</sup> I. Rico-lattes,<sup>§</sup> and W. Urbach<sup>||</sup>

Faculty of Pharmacy, University of Toronto, 19 Russell Street, Toronto, Ontario, Canada M5S 2S2, Laboratoire de Physique de la matière condensée, Collège de France, U.R.A 792 C.N.R.S., 5 Place Marcellin Berthelot, 75231 Paris cédex 05, France, Laboratoire des interactions moléculaires, réactivité chimique et photochimique, U.M.R. 5623 C.N.R.S., Université Paul Sabatier, 118 route de Narbonne, 31062 Toulouse, France, and Laboratoire de Physique Statistique, de l'Ecole Normale Supérieure, U.M.R. 8550 C.N.R.S., 24 rue Lhomond, 75231 Paris cédex 05, France

Received August 2, 2001. In Final Form: October 9, 2001

The behavior of a reverse lamellar phase has been studied by small-angle X-ray scattering upon the insertion of triblock molecules. A decrease of the lamellar spacing and membrane thickness was observed, whereas the Caillé exponent remained constant whatever the concentration of triblock molecules. A similar behavior was observed when surfactant molecules were added to the lamellar phase instead of triblock molecules. We demonstrate that our experimental results are consistent with the assumption that triblock molecules only participate to increase the membrane surface area. Moreover, we emphasize the fact that the surfactant molecular area varies with the membrane thickness. Indeed, this property appears to be the main effect causing the observed dramatic decrease of the lamellar spacing.

### Introduction

The change induced by inclusions to a lamellar phase depends on their location inside this lamellar phase as well as their interactions with the membrane (and hence of the structure of the inclusion). In the past decade, extensive studies have been performed on inclusions (i) dissolved in the solvent between the membranes (but not interacting with the membrane),<sup>1–3</sup> (ii) dissolved in the solvent of swollen membranes,<sup>4</sup> (iii) embedded into the membrane,<sup>5–7</sup> and (iv) absorbed on the membrane.<sup>8–10</sup> In

these previous studies, the inclusions are usually either completely hydrophobic or hydrophilic, and to a less extent amphiphilic. Recently, interest has been shown in triblock molecules, especially with hydrophilic/hydrophobic/hydrophilic structure. These inclusions induce spectacular behavior of the lamellar phase. For instance, triblock polymers induce phase transition<sup>11,12</sup> whereas triblock (transmembrane) protein and peptides exhibit molecular snap behavior<sup>13,14</sup> where the inclusions bind locally two membranes to each other. All these effects were induced by high molecular weight triblock molecules. So, we can wonder if these effects can also be induced by low molecular weight triblock molecules. Thus, in this article we propose to study the behavior of a reverse lamellar phase upon the insertion of low molecular weight triblock molecules.

### Materials and Methods

The triblock molecule (Scheme 1) consists of a mostly hydrophobic central part surrounded by two hydrophilic ends and has a molecular mass of 1172 g mol<sup>-1</sup>. The synthesis of the triblock molecule (Scheme 1) is performed by condensation of commercial 1,4,5,8-naphthalene tetracarboxylic dianhydride on *N*-(8-aminooctyl)-1-amino-1-deoxylactitol. This compound was obtained from lactose monohydrate and 1,8-diaminooctane; the synthetic procedure and the spectroscopic characteristics of *N*-(8-

\* To whom correspondence should be addressed.

† Faculty of Pharmacy, University of Toronto.

‡ Laboratoire de Physique de la matière condensée, Collège de France, U.R.A 792 C.N.R.S.

§ Laboratoire des interactions moléculaires, réactivité chimique et photochimique, U.M.R. 5623 C.N.R.S., Université Paul Sabatier.

|| Laboratoire de Physique Statistique, de l'Ecole Normale Supérieure, U.M.R. 8550 C.N.R.S.

(1) Ligoure, C.; Bouglet, G.; Porte, G.; Diat, O. Smectic compressibility of polymer-containing lyotropic lamellar phases: An experimental tool to study the thermodynamics of polymer confinement. *J. Phys. France* **1997**, *7*, 473–491.

(2) Bouglet, G.; Ligoure, C. Polymer-mediated interactions of fluid membranes in a lyotropic lamellar phase: a small-angle X-ray and neutron scattering study. *Eur. Phys. J. B* **1999**, *9*, 137–147.

(3) Singh, M.; Ober, R.; Kléman, M. Polymer in a lyotropic lamellar system: an experimental study. *J. Phys. Chem.* **1993**, *97*, 11108–11111.

(4) Radlinska, E. Z.; Gulik-Krzywicki, T.; Lafuma, F.; Langevin, D.; Urbach, W.; Williams, C. E. Modification of the lamellar phase in C12E5/water system by random hydrophilic–hydrophobic polyelectrolyte. *J. Phys. France II* **1997**, *7*, 1393–1416.

(5) Chen, C.-M. Theory for the bending rigidity of protein-coated lipid membranes. *Physica A* **2000**, *281*, 41–50.

(6) Netz, R.; Pincus, P. Inhomogeneous fluid membranes: segregation, ordering, and effective rigidity. *Phys. Rev. E* **1995**, *52*, 4114–4128.

(7) Taulier, N.; Gulik-Krzywicki, T.; Waks, M.; Urbach, W. Lateral interaction between transmembrane proteins embedded in thermally undulating lamella. *Eur. Lett.*, submitted.

(8) Clement, F.; Joanny, J.-F. Curvature elasticity of an absorbed polymer layer. *J. Phys. France* **1997**, *1*, 973–980.

(9) Bellocq, A.-M. Phase equilibria of polymer-containing micro-emulsions. *Langmuir* **1998**, *14*, 3730–3739.

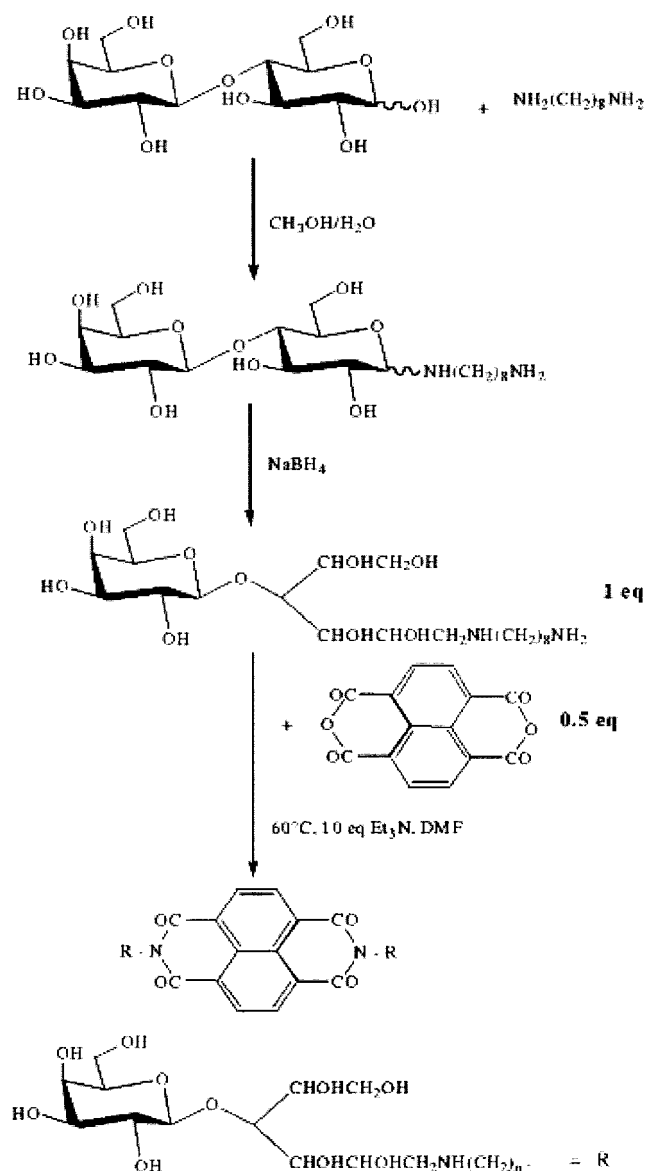
(10) Tsapis, N.; Ober, R.; Urbach, W. Dramatic rigidification of a peptide-decorated lamellar phase. *Phys. Rev. E* **2001**, *63*, 041903.

(11) Javierre, I.; Nallet, F.; A. Bellocq, M.; Maugey, M. Structure and dynamic properties of a polymer-induced sponge phase. *J. Phys.: Condens. Matter* **2000**, *12*, A295–A299.

(12) Taulier, N. Molecular snaps in a lamellar phase stabilized by steric interactions. Ph.D. Thesis, Université Paris 6, December 1999.

(13) Taulier, N.; Nicot, C.; Waks, M.; Hodges, R. S.; Ober, R.; Urbach, W. Unbinding-binding transition induced by molecular snaps in model membranes. *Biophys. J.* **2000**, *78*, 857.

(14) Nicot, C.; Waks, M.; Ober, R.; Gulik-Krzywicki, T.; Urbach, W. Squeezing of oil-surfactant bilayers by a membrane protein. *Phys. Rev. Lett.* **1996**, *77*, 3485–3488.

**Scheme 1. Graphical Summary of the Synthesis of the GFM13 Triblock Molecule (See Text)<sup>a</sup>**


<sup>a</sup> The structure of GFM13 is displayed at the bottom of the scheme, where the chain R is displayed separately.

aminoethyl)-1-amino-1-deoxylactitol have been described in a previous publication.<sup>15</sup> *N*-(8-Aminoethyl)-1-amino-1-deoxylactitol (1.2 mmol) was added to a solution of 1,4,5,8-naphthalene tetracarboxylic dianhydride (0.6 mmol) and 6 mmol of triethylamine in 50 mL of dimethylformamide. The mixture was stirred for 6 days at 60 °C. After evaporation of the solvent, the crude product was purified by chromatography on silica gel, eluting with a chloroform–methanol–30% ammonia solution (7:2.5:0.5). Yield, 7%. MS (FAB > 0, glycerol matrix/DMSO): 1173 (M+H)<sup>+</sup>, 1011 (M+H–Gal)<sup>+</sup>. The triblock macromolecule (GFM13 hereafter) is insoluble in pure water or dodecane. Tetraethylene glycol monododecyl ether (NIKKOL BL-4SY), denoted C<sub>12</sub>E<sub>4</sub>, was obtained from Nikko Chemicals Co. Ltd (Tokyo, Japan) and has a molecular mass of 362.55 g mol<sup>-1</sup>. Anhydrous dodecane was purchased from Aldrich Chemical Co. (Milwaukee, WI). Water was of the MILLIQ type (Millipore S.A., Molsheim, France).

The reverse lamellar phase was prepared by mixing the correct amount (added by weighting) of surfactant, dodecane, and water. A complete phase diagram of the tertiary system C<sub>12</sub>E<sub>4</sub>/dodecane/

(15) Rico-Lattes, I.; Gouzy, M.-F.; Andre-Barres, C.; Guidetti, B.; Lattes, A. Synthetic bolaamphiphilic analogues of galactosylceramide (galcer) potentially binding to the v3 domain of hiv-1 gp 120: key role of their hydrophobicity. *New J. Chem.* **1998**, *22*, 451–457.

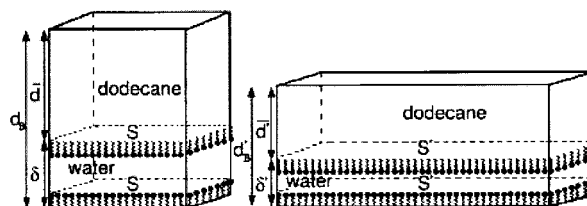


**Figure 1.** The cartoon shows that if the membrane surface increases ( $S' > S$ ) without change of solvent volumes ( $V = V$ ), then the lamellar spacing and the membrane thickness decrease, i.e.,  $d_B < d_B$  and  $\delta' < \delta$ .

water can be found in the article of Kunieda et al.<sup>16</sup> Each amount can be expressed by volume fraction  $\phi$ , which is the ratio of the volume of the considered component to the sample volume. The three volume fractions are dependent:

$$\phi_S + \phi_W + \phi_D = 1 \quad (1)$$

where suffixes S, W, and D are for surfactant, water, and dodecane, respectively. The resulting reverse lamellar phase is composed of a stack of lamellae separated by dodecane. Each lamella is formed by two monolayers of nonionic surfactant, C<sub>12</sub>E<sub>4</sub>, surrounding a layer of pure water (Figure 1). The sample remains in a reverse lamellar phase below 30 °C and becomes a reverse micellar phase above this temperature.<sup>17</sup> This property was used to insert triblock molecules inside the lamellar phase. The insertion protocol is the following: the reverse lamellar phase was first heated above 30 °C, and then GFM13 triblock molecules were added to the resulting reverse micellar phase. The solution was stirred until complete homogenization of the preparation was achieved. The sample was eventually cooled back at room temperature to a reverse lamellar phase.

To perform small-angle X-ray scattering (SAXS) experiments, the lamellar phase was transferred into Mark-Röhrchen capillaries (Hilgenberg GmbH, Malsfeld, Germany) of 1.5 mm diameter and sealed. The X-ray generator was a copper rotating anode machine operating at 40 kV and 25 mA. The X-ray apparent source had dimensions of 0.1 mm × 0.1 mm. A vertical mirror acts as a total reflector for the  $\lambda_{K\alpha} = 1.54 \text{ \AA}$  wavelength, eliminates shorter wavelengths of the beam, and directs the X-rays on the positive proportional counter. A nickel filter attenuates the  $\lambda_{K\alpha}$  wavelength. The dimensions of the beam on the counter were 3 mm vertically and 0.3 mm horizontally. The counter had a window of 3 mm height, a 50 mm useful length, and a 200  $\mu\text{m}$  spatial resolution. The distance between the sample and the counter was 802 mm. The measurements were carried out at 20–22 °C.

## Results

**Insertion of GFM13 Molecules.** In the following experiments, the initial composition of the reverse lamellar phase is  $\phi_S = 0.375$  and  $\phi_W = 0.217$  ( $\phi_D$  is then obtained from eq 1), with an initial ratio  $w = \phi_W/\phi_S = 0.58$ . Small-angle X-ray scattering experiments have been performed on the reverse lamellar phase with different concentrations of triblock molecules expressed as *R*, the molar ratio of triblock to surfactant molecules. The position,  $q_{\text{max}}$ , of the maximum of the first Bragg peaks in SAXS spectra (Figure 2) is related to the lamellar spacing (or Bragg distance) through  $d_B = 2\pi/q_{\text{max}}$ . All spectra have been fitted by the model of Nallet et al.<sup>18</sup> The fit gives the values of the polar

(16) Kunieda, H.; Nakamura, K.; Davis, H. T.; Evans, D. F. Formation of vesicles and microemulsion in water/tetraethylene glycol dodecyl ether/dodecane system. *Langmuir* **1991**, *7*, 1915–1919.

(17) Merdas, A.; Gindre, M.; Le Huérou, J.-Y.; Ober, R.; Nicot, C.; Urbach, W.; Waks, M. Bridging of noionic reverse micelles by a myelin transmembrane protein. *J. Phys. Chem. B* **1998**, *102*, 528–533.

(18) Nallet, F.; Laversanne, R.; Roux, D. Modelling X-ray or neutron scattering spectra of lyotropic lamellar phases: interplay between form and structure factors. *J. Phys. France II* **1993**, *3*, 487–502.

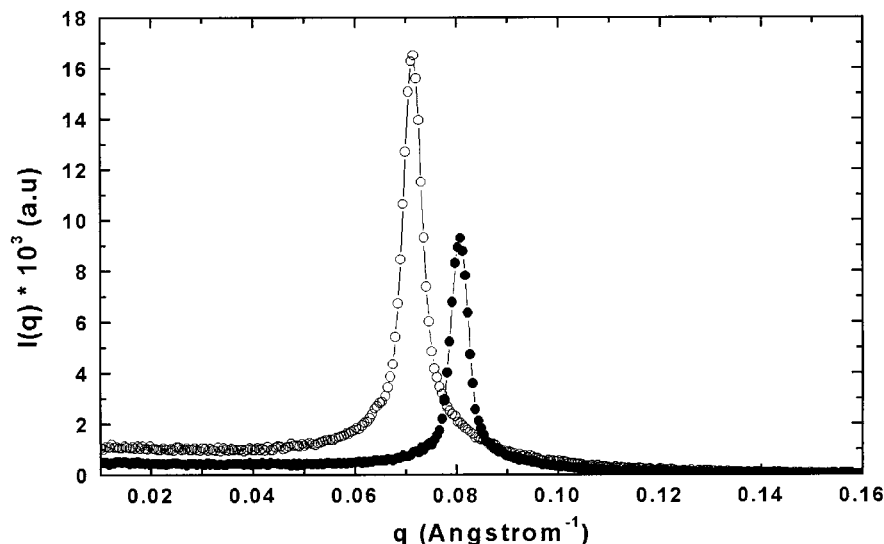


**Figure 2.** Spectra of the lamellar phase with (●,  $R = 15 \times 10^4$ ) and without (○,  $R = 0$ ) triblock molecules;  $\phi_S = 0.375$  and  $\phi_W = 0.217$ .

thickness of the membrane,  $\delta_{\text{polar}}$ , and the Caillé exponent  $\eta$ ,<sup>19</sup> which is related to the compressibility modulus,  $\bar{B}$ , and the rigidity modulus,  $K$ , of the lamellar phase through

$$\eta = \frac{\pi k_B T}{2d_B^2 \sqrt{KB}} \quad (2)$$

The membrane thickness,  $\delta$ , is eventually obtained by adding twice the length of the hydrophobic surfactant tail to  $\delta_{\text{polar}}$ , that is,  $\delta = \delta_{\text{polar}} + 2 \times 8 \text{ \AA}$ .

For  $R = 0$ , the lamella has a thickness equal to  $\delta \approx 52 \text{ \AA}$ , the initial interlamellar spacing,  $d_B$ , is approximately  $90 \text{ \AA}$ , and  $\eta \approx 0.32$ . The insertion of triblock molecules up to  $R = 15 \times 10^{-4}$  did not induce macroscopic phase transition. A well-defined peak of undulating lamellar phase was observed in the SAXS spectra (Figure 2), with no additional peaks that could reveal the presence of a coexisting microscopic phase or a substantial amount of defects.<sup>20,21</sup> When triblock molecules were added to the reverse lamellar phase, the Caillé exponent remained roughly constant and equal to 0.32 whatever the concentration of triblock molecules (Figure 3), while a decrease of the lamellar spacing from  $90$  to  $74 \text{ \AA}$  (Figure 4) and of membrane thickness from  $52$  to  $40 \text{ \AA}$  (Figure 5) was observed when  $R$  increased from  $0$  to  $15 \times 10^{-4}$ . Moreover, both decreases are linearly dependent on the triblock molecule concentration,  $R$ .

**Insertion of Surfactant Molecules.** To help us interpret the previous experimental data, we have performed the same kind of experiments but with the insertion of surfactant molecules,  $C_{12}E_4$ . In this case, we expect the surfactant molecules to enter the monolayers of the membrane. Note that the critical micellar concentration of  $C_{12}E_4$  is low,  $\sim 10^{-5} \text{ mol L}^{-1}$ .

In these experiments, the initial composition of the reverse lamellar phase is  $\phi_S = 0.278$  and  $\phi_W = 0.161$ . The initial ratio  $w = 0.58$  is the same as for the insertion of

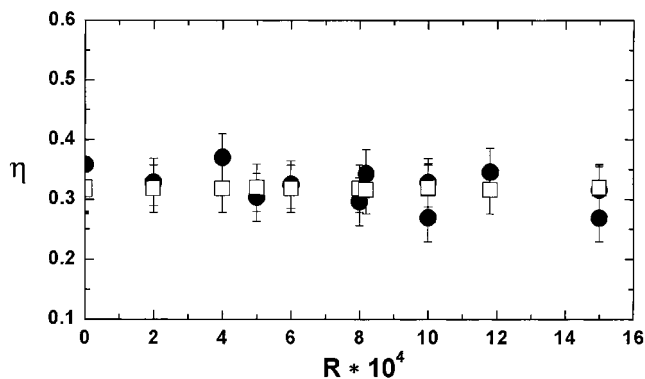


**Figure 3.** The Caillé exponent obtained from the fit of SAXS spectra (●) remains roughly constant around 0.32. Hollow squares (□) are values of the Caillé exponent calculated from the experimental values of  $d_B$  and  $\delta$  using eq 6 with  $\alpha = 2$ , see text.

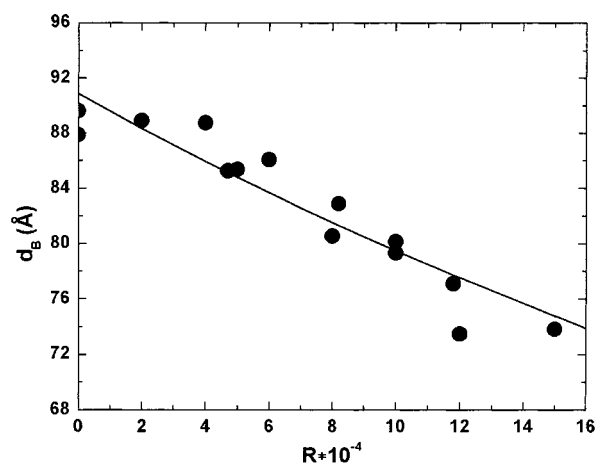


**Figure 4.** The lamellar spacing,  $d_B$ , versus the concentration,  $R$ , of triblock molecules. The continuous line is the fit obtained using eqs 9 and 10.

triblock molecules in order to get the same membrane thickness at the beginning of the experiment. Here again, no phase transition was observed and the SAXS spectra display only the well-defined peak of the lamellar phase (Figure 2) without the additional peak that could reveal the presence of a coexisting microscopic phase or of a

(19) Caillé, A. Remarques sur la diffusion des rayons x dans les smectiques a. *C. R. Acad. Sci. Paris* **1972**, *274b*, 891–893.

(20) Zipfel, J.; Berghausen, J.; Linder, P.; Richtering, W. Influence of shear on lyotropic lamellar phases with different membranes defects. *J. Phys. Chem. B* **1999**, *103*, 2841–2849.

(21) Holmes, M. C.; Smith, A. M.; Leaver, M. S. A small neutron scattering study of the lamellar phase of caesium pentadecafluorooctonate (CsPFO)/1H-1H-perfluoroheptan-1-ol/2H<sub>2</sub>O. *J. Phys. II France* **1993**, *3*, 1357–1370.

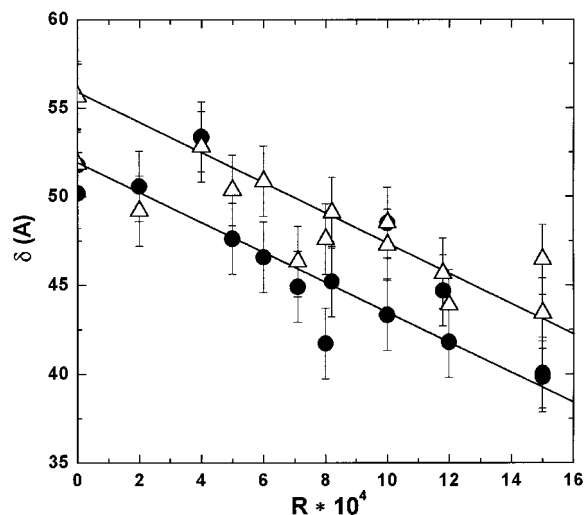


**Figure 5.** The experimental membrane thickness,  $\delta$ , decreases linearly with the concentration of triblock molecules (●). Hollow squares (□) are values calculated from the experimental values of  $d_B$  using eq 5. The lines indicate the general behavior of the experimental and theoretical data.

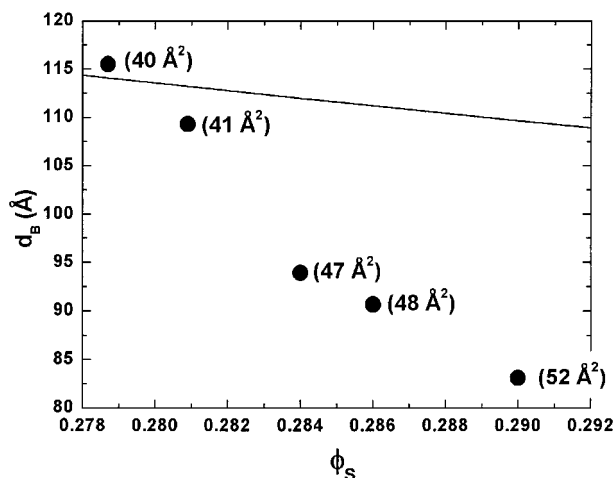


**Figure 6.** Each filled bullet represents an identical reverse lamellar phase except for the number of surfactant molecules, which is given by the surfactant volume fraction,  $\phi_s$ . The calculated surfactant molecular area (see text) is displayed near the bullet. The line represents the value that  $d_B$  would take if the molecular area remained constant and equal to  $40 \text{ \AA}^2$ .

substantial amount of defects. The values of the lamellar spacing (Figure 6) and membrane thickness (Figure 7) decreased with the addition of surfactant molecules, expressed through the volume fraction of surfactant,  $\phi_s$ . The Caillé exponent is constant and equal to  $0.63 \pm 0.4$  (figure not shown) whatever the addition of surfactant molecules.

### Discussion

The observed behavior of the reverse lamellar phase should strongly depend on the location of the inclusions. Since there is no direct method to determine the exact location of triblock molecules, we can only form a hypothesis on their location and verify that the expected effects are effectively observed in our experiments.

The fact that GFM13 triblock molecules are insoluble in pure oil or water definitively helps us to assert that in the lamellar phase they are absent from the oil or from the water. Furthermore, if GFM13 molecules were dissolved in oil (or water) the total membrane surface should

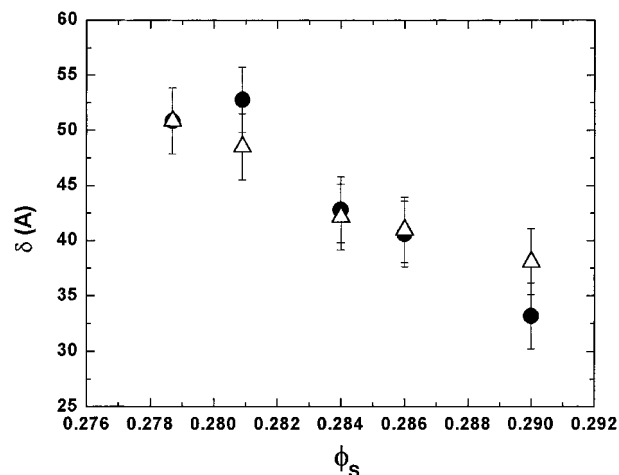


**Figure 7.** The experimental membrane thickness (●) decreases when surfactant molecules are added to the lamellar phase. The experimental data are in good agreement with the predicted values (△) calculated from eq 5.

be constant and the lamellar spacing should not vary (since the sample volume weakly changes due to the negligible addition of the triblock molecules' volume), which is obviously not observed in our experiments. Possibilities of other locations are few. Triblock molecules could be bound to the surface of the monolayers. In this situation, we expect no change of  $d_B$  but an increase of membrane rigidity and hence a decrease of  $\eta$ .<sup>10,22</sup> Or inclusions could act as molecular snaps. In that case, formation of molecular snaps induces a phase transition and a lamellar spacing which behaves as  $d_B \approx R^{-0.5}$ .<sup>13</sup> For both previous cases, the expected behavior is completely different from what was observed in our samples.

Finally, since no phase transition or formation of defects is observed, we are left with the hypothesis that triblock macromolecules are somehow inserted into the monolayers of the membrane. Indeed, this assumption seems reasonable considering that the behavior of the lamellar phase (i.e., of  $d_B$ ,  $\delta$ , and  $\eta$ ) is the same when GFM13 or surfactant molecules are inserted. Namely, for both cases we observed a decrease of the same order of membrane thickness,  $\delta$ , and lamellar spacing,  $d_B$ , and values of the Caillé exponent,  $\eta$ , remain constant whatever the addition of inclusions. We will show hereafter that a model describing the insertion of inclusions in the monolayers of the membrane successfully describes the observed behavior of  $d_B$ ,  $\delta$ , and  $\eta$  when triblock or surfactant molecules are used.

**Model.** From geometrical considerations (Figure 1), the lamellar spacing,  $d_B$ , and the membrane thickness,  $\delta$ , can be related to the total membrane surface,  $S$ :

$$d_B(R) = \frac{V}{S} \quad (3)$$

$$\delta = \frac{v_m}{S} \quad (4)$$

where  $V$  and  $v_m$  are the sample and membrane volumes, respectively. For high oil dilution,  $S$  should be replaced in eq 3 by the projected membrane surface,  $S_p$ , to take into account the membrane thermal undulations.<sup>23</sup> But at the low lamellar spacing used here, this correction is negligible, that is,  $S \approx S_p$ . For convenience, we use eq 3

(22) Sens, P.; Turner, M. S. Structure factor of a lamellar smectic phase with inclusions. *Eur. Phys. J. E* **2001**, *4*, 115–120.

(23) Helfrich, W. Effect of thermal undulations on the rigidity of fluid membranes and interfaces. *J. Phys.* **1985**, *46*, 1263–1268.

to rewrite eq 4 as

$$\delta = \frac{V_m}{V} d_B = (\phi_S + \phi_D) d_B \quad (5)$$

It has been already shown that the reverse lamellar phase under study is stabilized by steric interactions<sup>13</sup> and that the Caillé exponent follows the classical law:<sup>24</sup>

$$\eta = \alpha \left(1 - \frac{\delta}{d_B}\right)^2 \quad (6)$$

The total membrane surface area,  $S$ , depends of the number of moles of surfactant molecules,  $N_S$ , as well as the surfactant molecular area,  $a_S$ :

$$S = \frac{N_S \mathcal{N} a_S}{2} \quad (7)$$

where  $\mathcal{N}$  is the Avogadro number. If  $N_i$  moles of inclusions are inserted in the monolayers, then the membrane surface area is modified as

$$S = \frac{N_S \mathcal{N}}{2} (a_S + R a_i) \quad (8)$$

where  $R = N_i/N_S$  and  $a_i$  is the molecular area of inclusions.

Therefore, if the inclusions increase the membrane surface area as described by eq 8, the lamellar spacing should decrease according to

$$d_B(R) = \frac{2V}{N_S \mathcal{N} (a_S + R a_i)} \quad (9)$$

In the meantime, the membrane thickness should also decrease according to eq 5. For low concentration ( $R < 10^{-2}$ ), the contribution of inclusions to volumes (i.e.,  $V$  and  $v_m$ ) is negligible in eqs 9 and 5. Since volumes can be considered as constant, the ratio  $\delta/d_B$  (eq 5) and therefore the Caillé exponent (eq 6) should be constant whatever the concentration of inclusions.

In conclusion, the previous model allows the calculation of the lamellar spacing using eq 9. Then, values of  $d_B$  can be used to derive the membrane thickness using eq 5, and  $d_B$  and  $\delta$  are eventually used to derive the Caillé exponent using eq 6. Unfortunately, both surfactant and triblock molecular areas are unknown, so the lamellar spacing cannot be predicted. But the fit of the experimental values of  $d_B$  by eq 9 allows the extraction of the molecular areas  $a_S$  and  $a_i$ . Moreover, the experimental values of  $d_B$  can be used to derive the membrane thickness,  $\delta$ , and Caillé exponent,  $\eta$ .

#### Application to Surfactant Molecules as Inclusions.

To validate this model and to determine the value of  $a_S$ , we use the experimental data performed when surfactant molecules ( $C_{12}E_4$ ) have been used as inclusions (i.e.,  $a_i = a_S$ ). Indeed, in such a case surfactant molecules undoubtedly increase the membrane surface area. Figure 6 shows that the behavior of the membrane thickness is effectively in good agreement with eq 5 and that the Caillé exponent is constant as expected and equal to  $0.63 \pm 0.4$  (figure not shown).

Using eqs 3 and 7, the values of the surfactant molecular area are calculated from the lamellar spacing (the values are displayed in Figure 6). We observe that  $a_S$  increases

from 40 to 52 Å<sup>2</sup> when  $\phi_S$  increases from 0.278 to 0.29. To emphasize the effect of the change of surfactant molecular area on the lamellar spacing, we have plotted the numerical values of  $d_B$  for the case where  $a_S$  would remain constant and equal to 40 Å<sup>2</sup> (continuous line in Figure 6). The reason the surfactant molecular area varies is undetermined. However, from previous oil-dilution experiments<sup>13</sup> (i.e., when  $S$  and  $\delta$  are kept constant and  $V$  varies) we know that a change in the lamellar spacing does not affect the surfactant molecular area. Consequently, we suggest that the increase in molecular area is due to the decrease in lamellar thickness. We effectively observe that the surfactant molecular area depends linearly on the membrane thickness:

$$a_S \approx c_1 \delta + c_2 \quad (10)$$

where  $c_1 = -0.52 \pm 0.05$  and  $c_2 = 68 \pm 2$ . So we can hypothesize that the larger proximity of surfactant molecules reduces their entropic motion and that surfactant molecules reduce this constraint by increasing their surfactant molecular area.

Moreover, we pointed out that the oil-dilution experiments exhibit the behavior of a classical lamellar phase. This shows that no defects are present in our system,<sup>25</sup> which is confirmed by previous freeze-fracture electron microscopy experiments done on the system.<sup>7,14</sup>

Consequently, the model succeeds in describing the behavior of the lamellar spacing, membrane thickness, and Caillé exponent provided that we take into account the change in surfactant molecular area with the membrane thickness as described by eq 10. Thus, our model should be composed of eqs 5, 6, 9, and 10.

#### Applications to Triblock Molecules as Inclusions.

We first calculate the values of the membrane thickness from the experimental values of  $d_B$  using eq 5 and then the values of the Caillé exponent from the experimental values of  $\delta$  and  $d_B$  using eq 6. We observed that both numerical values of  $\delta$  and  $\eta$  follow the same behavior as their respective experimental values (Figures 5 and 3). A difference of up to 3 Å is observed between experimental and numerical values of  $\delta$  (Figure 5), whereas a value of  $\alpha$ , in eq 6, has been taken to 2 in order to get the same value as the experimental one (Figure 3). The value of  $\alpha$  should be equal to 1.33 according to the theoretical model of Helfrich,<sup>26</sup> but higher values (between 1.4 and 2.4<sup>12</sup>) were always found for reverse oil-swollen lamellae.

Then, the experimental values of the lamellar spacing have been fitted using eq 9 (Figure 3). The value of  $a_i$  in eq 9 is used as an unknown parameter. And values of  $a_S$  are replaced by eq 10, where  $\delta$  is the experimental value of the membrane thickness and  $c_1$  and  $c_2$  are also considered as unknown parameters. We find that  $a_i \approx 400$  Å<sup>2</sup>, which is a reasonable value for the molecular area of triblock molecules, and  $c_1 = 0.57 \pm 0.05$  and  $c_2 = 67 \pm 1$  for the change in surfactant molecular area. Note that we have supposed for simplicity that  $a_i$  is constant, but we can easily imagine that  $a_i$  also varies with the membrane thickness. If this is effectively the case, the change in  $a_i$  should be reflected in  $a_S$  in our model. That could explain the difference found in the slope  $c_1$  in eq 10 between surfactant and triblock molecules.

Finally, note that the membrane rigidity,  $\kappa = K/d_B$ , did not appear in our model. That does not mean that  $\kappa$  is

(25) Berger, K.; Hiltrop, K. Characterization of structural transitions in the SLS/decanol/water system. *Colloid Polym. Sci.* **1996**, *274*, 269–278.

(26) Helfrich, W. Steric interaction of fluid membranes in multilayer systems. *Naturforsch. Z. A* **1978**, *33*, 305–315.

(24) Roux, D.; Safinya, C. R. A synchrotron X-ray study of competing undulation and electrostatic interlayer interactions in fluid multilayer membrane lyotropic phases. *J. Phys. France* **1988**, *49*, 307–318.

constant. In fact, we expect that  $\kappa$  increases when the membrane thickness decreases. Additionally, we expect the monolayer rigidity,  $\kappa_{\text{mono}}$ , to be weakly affected by the presence of surfactant or GFM13 inclusions. Indeed, the rigidity of GFM13 triblock molecules should be of the same order as that of surfactant molecules.

### Conclusion

We have shown that the insertion of triblock molecules into a reverse lamellar phase induces a decrease of the interlamellar spacing and membrane thickness. Both observables decrease linearly with the same slope, which is reflected in the fact that the Caillé exponent is constant whatever the addition of inclusions. A similar behavior is also observed when surfactant molecules are used instead of triblock molecules. These effects are mainly due to an indirect and cooperative mechanism from surfactant molecules. Specifically, triblock molecules are inserted in the surfactant monolayers and contribute to increase the

membrane surface area,  $S$ , which in turn decreases the membrane thickness,  $\delta$ . Surfactant molecules are sensitive to this decrease and respond to this effect by increasing their molecular area,  $a_s$ . The increase of surfactant molecular area leads to a further increase of the membrane surface and consequently to a significant decrease of the interlamellar spacing. We have shown that this effect also happens with the addition of surfactant molecules, and in general we expect this behavior for any molecules which enter the surfactant monolayer. The decrease of the interlamellar spacing is significant for a low amount of inclusions (one inclusion for 1000 surfactant molecules). Consequently, when the membrane thickness varies, it is necessary to take into account the related change of molecular area per surfactant, since a small variation of this molecular area induces a dramatic change of the interlamellar spacing.

LA0155202